Kinetics Profile of Hybridoma Clones SB4 and RD8 Producing Monoclonal Antibodies Against The Spike Protein Of SARS-Cov-2 In Low-Serum Medium

Indri FEBRIANI[1,2], Febby Nurdiya NINGSIH[1,*], Sri Rahayu LESTARI[2], Jodi SURYANGGONO[1], Erba Vidya CIKTA[3], Tika WIDAYANTI[1], Asri SULFIANTI[1], R. Tedjo SASMONO[4], Sabar PAMBUDI[1]

[1]Research Center for Vaccine and Drugs, National Research and Innovation Agency, South Tangerang, Banten, Indonesia; [2]Department of Biology, Faculty of Mathematics and Natural Sciences, Universitas Negeri Malang, Malang, East Java, Indonesia; [3]Center of Pharmaceutical and Medical Technology, Agency for the Assessment and Application of Technology (BPPT), Serpong, South Tangerang, Indonesia; [4]Eijkman Research Center for Molecular Biology, National Research and Innovation Agency, Cibinong Science Center, Cibinong, West Java, Indonesia

Abstract

Background. Monoclonal antibodies, the main component of antigen-based rapid diagnostic tests, are produced in vitro through hybridoma cell cultivation supplemented with animal-derived serum, such as fetal bovine serum. The supplementation of FBS in culture medium causes controversy due to the variation of components included in FBS per production, potentially reducing the quality of mAbs. Moreover, the cost of using FBS is high. This study aimed to evaluate the growth capacity of hybridoma clones after being adapted to low serum conditions.

Methods. The clones SB4 and RD8 producing mAb against spike protein of SARS-CoV-2 were used in this study. Cell kinetics were observed and measured for seven days with 10% and 3% FBS supplementation. Then, the mAbs production was measured semi-quantitatively by indirect enzyme-linked immunosorbent assay. In addition, the cell cycle was also evaluated through flow cytometry analysis at 24 h, 48 h, and 72 h of treatment. This study was conducted with a true-experiment method (n=3), and all quantitative results were statistically analyzed.

Results. The results show that supplementation of 3% FBS in these two hybridoma clones gave a different response regarding cell proliferation and productivity. The clone RD8 was excellent in growth kinetics and maintained the mAbs production on low-serum media, while SB4 showed a different pattern.

Conclusion. Accordingly, supplementation of 3% FBS may support hybridoma productivity as a fulfilment of mAbs production while considering the characteristics of each hybridoma clone.

Keywords: monoclonal antibody, rapid diagnostic test, hybridoma cells, fetal bovine serum

1. Introduction

Monoclonal Antibodies (mAbs) are widely commercially used for research, diagnosis, and therapeutics. Therapeutically, mouse-mAbs can be modified into human-mouse chimeric forms for cancer, autoimmune, and degenerative disease treatments (Fesseha, 2020; Sánchez-Robles *et al.*, 2021). In COVID-19 Rapid Diagnostic Tests (RDTs), the antigen-antibody reaction, particularly for detecting the spike protein of SARS-CoV-2, relies on mAbs as essential raw materials (Salcedo *et al.*, 2022). Therefore, efficient mAbs production is critical. Produced by hybridoma cells from the fusion of splenocytes and myeloma cells, mAbs can be generated either in vitro (bioreactors) or in vivo (ascites). Due to considerations of scale, cost, ethics, and the 3R (Replace, Reduce, Refine) principle, the in vitro method is preferred (Khan, 2023; Verderio *et al.*, 2023).

Monoclonal antibodies produced by hybridoma are influenced by the supplementation of growth factors that affect metabolic rates (Sissolak et al., 2019). This process typically uses media supplemented with Fetal Bovine Serum (FBS) in bioreactors or spinner flasks. FBS is a source of vital cell nutrients, such as growth factors, hormones, and amino acids. Thus, its role remains essential and intricate, but its use is controversial due to ethical concerns, contamination risks (Versteegen *et al.*, 2021), quality variability, and purification challenges (Groothuis *et al.*, 2015; Baker, 2016; Urzì *et al.*, 2022). These issues have encouraged researchers to avoid serum usage in hybridoma culture medium.

Although a study by Hashmi *et al.* (2014) showed low mAbs production after cultivation in a medium supplemented with 0.5% FBS, the kinetic profile of the cells was not well evaluated. Thus, we assume that 0.5% FBS supplementation is insufficient to support hybridoma in producing mAbs. Additionally, there is a possibility that

---

* Corresponding author. e-mail: febb001@brin.go.id.

each clone may respond differently to nutritional changes. Therefore, this study compares the growth capacity of two generated hybridomas, clones SB4 and RD8, in response to supplementation with 3% FBS versus 10% FBS. Assessing the cell kinetics after sequential adaptation to low-serum supplementation is required to estimate mAbs production and the optimum period needed. Through this study, we expect to explain the growth profile of clones SB4 and RD8 in culture media with low FBS content. Thus, this study will form the basis for establishing the hybridoma clone with a high capacity of mAbs production.

2. Materials and methods

2.1. Design of experiment

This study is a true experiment and was conducted in at least three independent experiments. Both control and treatment groups were done with three replications, respectively (n = 3).

2.2. Hybridoma cell lines and cell cultivation

Hybridoma cell clones SB4 and RD8 were developed at the Research Center for Vaccine and Drugs, Indonesia. Both clones are confirmed to produce the mouse monoclonal antibody against the Spike Recombinant Protein of SARS-CoV-2 (unpublished data). Hybridomas were adapted in RPMI-1640 growth medium (Gibco^{TM}, USA) with FBS supplementation starting at 10% then gradually reduced to 8%, 5%, and finally, 3% (Sigma®, St. Louis, MO, USA), along with 100 U/mL penicillin-streptomycin (Gibco^{TM}, USA). Each clone was cultivated in a 25 cm² T-flask and then incubated at 37°C with 5% CO_2 following a similar procedure (Parveen and Varalakshmi, 2022; Loniakan *et al.*, 2023). Medium replacement was performed every 2–3 days, while subculture into a large-sized flask was accomplished when cell confluence reached ~70–80%.

2.3. Measurement of growth kinetics of hybridoma cells

The protocol is based on the studies by Bruce *et al.* (2002) and Silva *et al.* (2018), with adjustments and slight modifications of methods. Adapted hybridoma cell clones SB4 and RD8, in RPMI medium supplemented with 3% FBS, were subcultured into Durant bottles equipped with magnetic stirrers. The initial cell density cultivated was 1 x 10⁵ cells/mL, using a batch culture system with a working volume of 70 mL. As a comparator, clones established in a medium containing 10% FBS were cultivated and measured in parallel. Culture samples from days 1 to 7 were collected, with 1 mL for microscopic observation and 500 μL (n = 3) for cell count calculation according to Khalil (2009)**.** Based on the cell numbers determined by culture sampling on days 1 to 7, population doubling time (PDT) and growth rate were calculated using an equation or measured via the OMNI calculator website (https://www.omnicalculator.com/biology/cell-doubling-time).

$$PDT = \frac{\Delta t}{log2\left(\frac{\Delta N}{N0}\right)+1}$$ (Korzyńska & Zychowicz, 2008)

PDT　　　= Population doubling time
Δt　　　　= Time taken for 80% confluency
ΔN　　　= Difference in cell number or concentration
N0　　　　= Total cell number seeded or concentration

$$Growth\,rate = \frac{ln\left(\frac{N2}{N1}\right)}{t2-t1}$$ (Singer & McDaniel, 1986)

N or W　　= Cell number or concentration
N2　　　　= Final cell number or concentration
N1　　　　= Initial cell number or concentration
t　　　　　= Time

The samples collected from days 1 to 7 were centrifuged, with the supernatant stored at 4°C as a daily mAbs production sample, while the cell pellets were fixed using 70% ethanol (proceed to sub-section 2.5). After day 7, all cultures were harvested by centrifugation to separate the supernatant from the cells. The supernatants containing mAbs were concentrated with Amicon® Ultra Centrifugal Filters 100 kDa MWCO (Merck, Germany) and then stored at -20 °C (Proceed to sub-section 2.6).

2.4. Measurement of monoclonal antibody production by indirect ELISA

The mAbs absorbance measurement protocol refers to the study by Ningsih *et al.* (2023), with adjustments and modifications of methods. A CoronaVac antigen 50 ng/well (Biofarma, Indonesia) and non-structural SARS-CoV-2 proteins (50 ng/well, n=3) produced by the Research Center for Vaccine and Drug, Indonesia, were used as negative controls. These were coated on the Nunc MaxiSorp™ 96-well high-binding microplate (Thermo Scientific, USA) and incubated overnight at 4°C. Samples were then washed with 100 μL/well of phosphate-buffered saline containing 0.1% Tween-20 (PBS-T 0.1%) six times (placed on a shaker for five minutes). Next, samples were incubated for four hours with a blocking buffer containing 5% BSA (Sigma, USA) and then rinsed three times with PBS-T 0.1% in the same manner as previously.

A supernatant sample was used as the tested primary antibody (150 μL/well), a RPMI medium containing FBS was used as a negative control, and a monoclonal antibody against SARS-Cov-2 Spike protein S1 (Cat MA5-36250, Invitrogen, USA) was used as a positive control. After overnight incubation at 4°C, samples were washed with PBS-T 0.1% eight times before being incubated for an hour with a secondary antibody against mouse-conjugated stabilized peroxidase (Cat. 626520, Invitrogen, USA) for the supernatant sample and negative control, and HRP-conjugated goat anti-rabbit (Cat. GTX213110-01, Invitrogen, USA) for the positive control. Next, the samples were washed using PBS-T 0.1% eight times before being incubated for 15 minutes with a 50 μL/well of 1-Step^{TM} Ultra TMB-ELISA (Thermo Scientific, USA). Then, 50 μL/well of H_2SO_4 0.5 N was added to all samples to stop the reaction. Lastly, the optical density at 450 nm was measured using a Synergy HTX Multi-Mode Reader (Agilent Technologies, USA).

2.5. Analysis of cycle cell by flow cytometry

The fixed cells at 24 h, 48 h, and 72 h (n = 3) were centrifugated and washed with sterile PBS 1X. Then, the cells were stained with propidium iodide (PI) solution (Invitrogen, USA) containing RNase A (Sigma, USA) and incubated for 15 minutes (dark condition). Finally, cell

cycle analysis on each sample from both clones was performed using BD AccuriTM C6 Plus flow cytometry (BD Biosciences, USA). A PI solution without a sample is used as a blank. The setting limitations included 10,000 events, medium fluidics velocity, and a threshold of 80,000 on FSC-H.

2.6. Qualitative total protein profiling

The total protein in both mAbs concentrate and flowthrough samples obtained from the previous step (Sub-section 2.3) was quantified using Pierce™ BCA Protein Assay Kits (Thermo Scientific, USA) compared to albumin as the standard. The absorbance was measured at a wavelength of 562 nm.

Then, the protein profile of each sample was analyzed by sodium dodecyl sulphate-polyacrylamide gel electrophoresis (SDS-PAGE) using a 10% polyacrylamide resolving gel. All samples were diluted with 5X loading dye and adjusted to 1 mg total protein in a final volume of 20 μL, then run with Electophoresis WSE-1150 PageRun Ace (Atto, Japan) for at least 90 minutes. A PageRuler™ Plus prestained protein ladder was used as the size indicator (Thermo Scientific, USA). The bands were visualized with Coomassie Brilliant Blue R-250 staining solution (Bio-Rad, USA) followed by a destaining solution (Bio-Rad, USA).

2.7. Statistical analysis

The reported data represent three independent experiments with similar findings and are presented as geometric means ± standard deviations (SD). The normality of all data was tested using Shapiro-Wilk and Levene homogeneity tests. A Mann-Whitney non-parametric test was conducted to compare the differences between 10% and 3% FBS supplementation on all parameters tested for both clones. This test is used in in vitro research by Saleh *et al.* (2021). A *p*-value of less than 0.05 was considered statistically significant. The statistical analysis software used was SPSS version 25, while the graphs were created using Microsoft Excel.

3. Results

3.1. Kinetics of growth and production of monoclonal antibodies (mAbs) by hybridoma clones SB4 and RD8 after adaptation to low-serum medium

This study uses the spike protein of SARS-CoV-2 at the ELISA coating plate stage to test cross-reactivity with commercial mAbs (as a positive control system) and mAbs in the supernatant sample. The ELISA system has been optimized and well-verified.

Figure 1A shows the growth kinetics of hybridoma clone SB4. In media supplemented with 3% FBS, clone SB4 reached the highest density on day 3, approximately $483,970 \pm 76,610$ cells/mL. This value is less than the total viable cells cultivated in media with 10% FBS, yet statistically not significantly different ($p > 0.05$). The PDT and growth rate calculation also support this result. Clone SB4 supplemented with 3% FBS showed a longer PDT than 10% FBS, resulting in a slower growth rate.
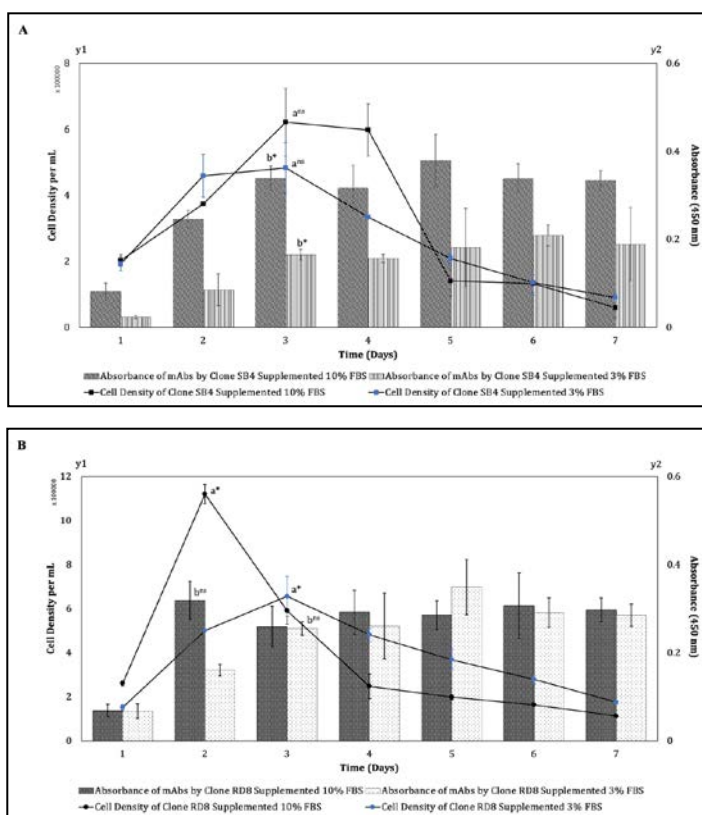
Figure 1. Kinetics of cell growth and mAbs production by hybridoma cells for seven days. (A) Hybridoma clone SB4. (B) Hybridoma clone RD8. The values are presented as geometric mean ± Standard Deviation (SD, n = 3), compared to negative and positive control. The value of the bar considered as the peak for [a)]Viable cell density and [b)]mAbs production, were analyzed using the Mann-Whitney test and presented as [ns)]not significantly different ($p > 0.05$); [*)]significantly different (p < 0.05).

The density reduction in media supplemented with 3% FBS also occurred in clone RD8. Figure 1B shows RD8 reached the highest density in 3% FBS on day 3, approximately 656,764 ± 91,320 cells/mL. This value decreased significantly by half compared to the sample cultivated in 10% FBS, which was 1,120,582 ± 43,989 cells/mL on day 2. Additionally, the highest density of clone RD8 with supplementation of 10% FBS also grew faster than in 3% FBS. Meanwhile, the decrease in viable cell number of clone SB4 with 3% FBS was supported by a longer PDT and slower growth rate (see Table 1) but was statistically insignificant. The density and morphological condition of both clones during supplementation with 3% FBS at the end of the log phase are visualized by microscopic observations in Figure 2. The cell density in media supplemented with 3% FBS was less than the cells cultivated with 10% FBS.
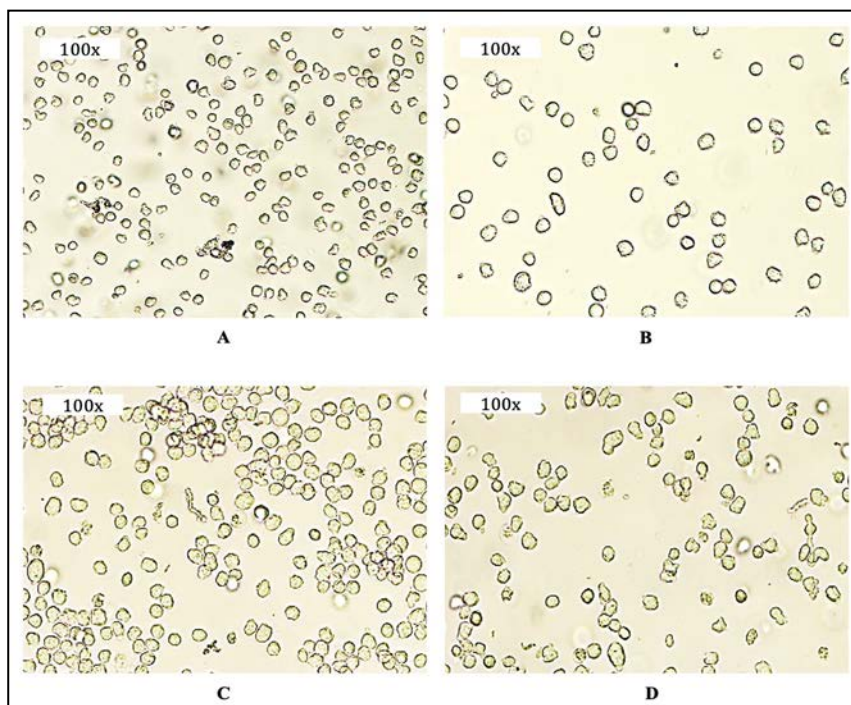
Figure 2. Microscopic observation of hybridoma clones SB4 and RD8 on peak cell density days (100× magnification). One millilitre sample from each culture was collected and placed on the dish. Cell observation of clone SB4 supplemented with (A) 10% FBS on day 3; (B) 3% FBS on day 3. Clone RD8 supplemented with (C) 10% FBS on day 2; (D) 3% FBS on day 3. The figures shown are representative of experiments that showed similar results.

In Figure 1A, based on the relative absorbance level of mAbs, the highest peak of mAbs production by SB4 cells with 3% FBS on day 3 was approximately 0.165 ± 0.011. These values decreased by half compared to supplementation with 10% FBS, which was 0.340 ± 0.027 (significant decrease). The peak absorbance of these clone SB4 mAbs occurs on the day of the peak cell density. Similarly, in the graph of mAbs production by clone RD8 (Figure 1B), the peak of mAbs production also occurred on the peak day of cell density, which is day 3 for RD8 with 3% FBS, at 0.256 ± 0.016. These values are still less than the mAbs production with 10% FBS, which was 0.318 ± 0.04 on day 2 (insignificant decrease).

3.2. Comparison of competence of clones SB4 and RD8 on low-serum medium

In Table 1, the peak growth density of clone RD8 with 3% FBS is still less than that of clone SB4 (difference not significant). However, clone RD8 supplemented with 3% FBS showed a more significant peak of mAbs production than clone SB4, which were 0.256 ± 0.016 and 0.165 ± 0.011, respectively (statistically significant difference).

Table 1. Summary table of growth kinetics and production of mAbs by clones SB4 and RD8 supplemented with 10% and 3% FBS.

| Parameters	Clone SB4		Clone RD8	
	10% FBS	3% FBS	10% FBS	3% FBS
Highest density	On day 3 (622,269 ± 103,175 cells/mL)	On day 3 (483,970 ± 76,610 cells/mL)	On day 2 (1,120,582 ± 43,989 cells/mL)	On day 3 (656,764 ± 91,320 cells/mL)
Highest mAbs production	On day 3 (0.340 ± 0.027)	On day 3 (0.165 ± 0.011)	On day 2 (0.318 ± 0.043)	On day 3 (0.256 ± 0.016)
PDT in lag phase–exponential phase	On day 1–3 (29 hours 46 minutes)	On day 1–3 (36 hours 12 minutes)	On day 0–2 (13 hours 46 minutes)	On day 1–3 (22 hours 48 minutes)
Growth rate	On day 1–3 (0.023)	On day 1–3 (0.019)	On day 0–2 (0.050)	On day 1–3 (0.030)

3.3. Decreased FBS levels in the growth medium affect the cell cycle of clones SB4 and RD8

As shown in Figure 3, the percentage of the SB4 cell population in the sub-G1 phase in both FBS contents gradually increased from 24 h to 72 h. Clone SB4 supplemented with 3% FBS tended to have a smaller proportion of dead cells (sub-G1 phase) than cells cultivated with 10% FBS, approximately 9.81 ± 1.40 % and 14.15 ± 0.79 %, respectively (insignificant, $p > 0.05$).

In the S phase, the proportion of SB4 cells supplemented with 3% and 10% FBS from 24 h to 72 h tended to decrease gradually. At 24 h, the relative number of proliferating cells (G2/M) observed in 3% FBS was lower than in 10% FBS. Interestingly, at 72 h, the proportion of G2/M phase cells observed in 3% FBS was approximately four times higher than that in 10% FBS ($p > 0.05$). After 72 h, SB4 cells in medium with 3% FBS had a smaller population proportion of sub-G1 (dead cells) and a higher proportion of G2/M phase (proliferating cells) than those in 10% FBS.
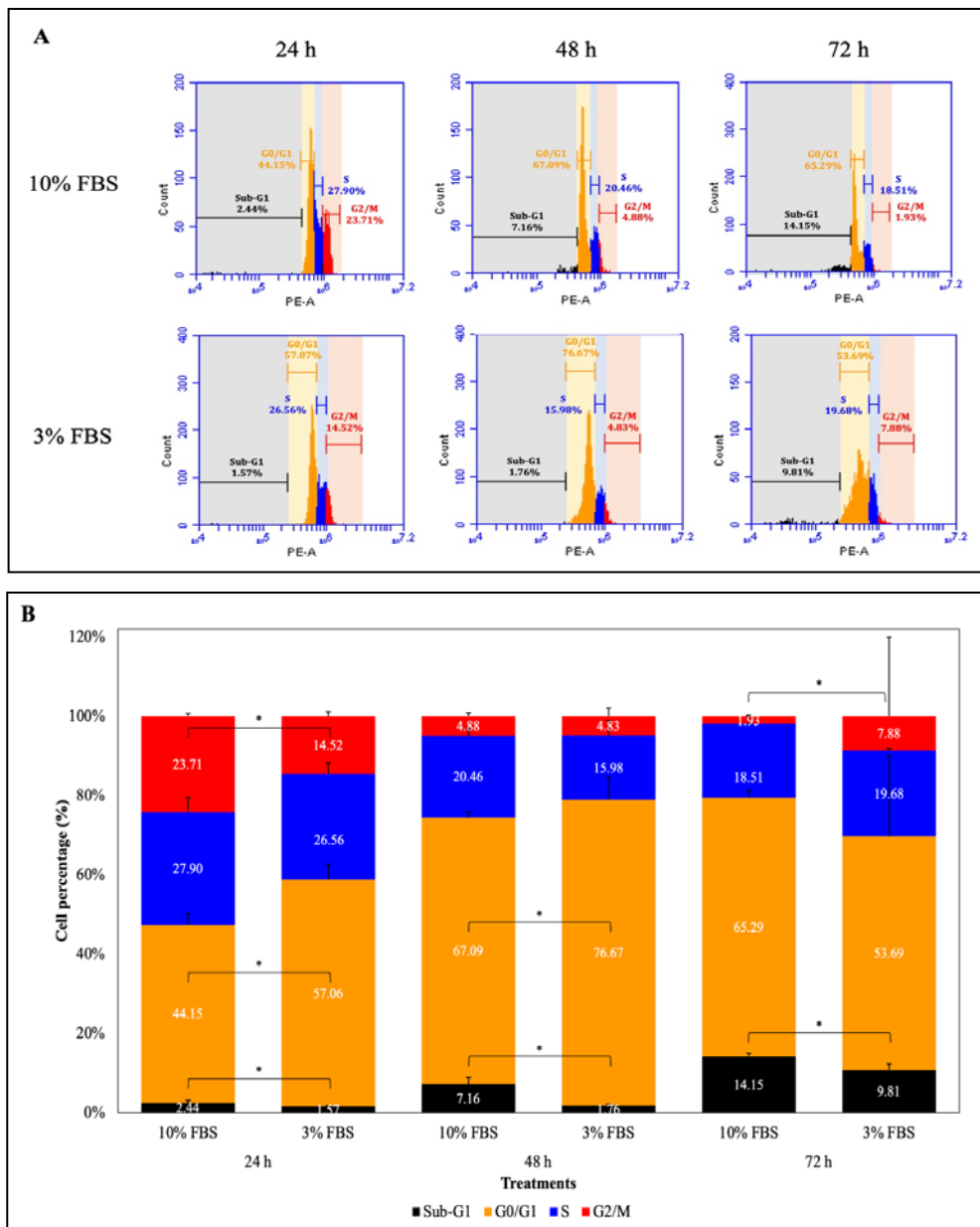
Figure 3. The cell cycle of clone SB4 supplemented with 10% and 3% FBS (n = 3). A. Flow cytometry-based cell cycle spectrum at 24 h, 48 h, and 72 h treatment. B. Cell percentage bar chart per phase at 24 h, 48 h, and 72 h of treatment. The percentage value is the geometric mean, and the system control value already subtracts the relative percentage of cells. The cell cycle spectrum of hybridoma is divided into Sub-G1, G0/G1, S, and G2/M phases with different colour representatives. Cell cycle data were also statistically analyzed using the Mann-Whitney test. *(p ≤ 0.05).
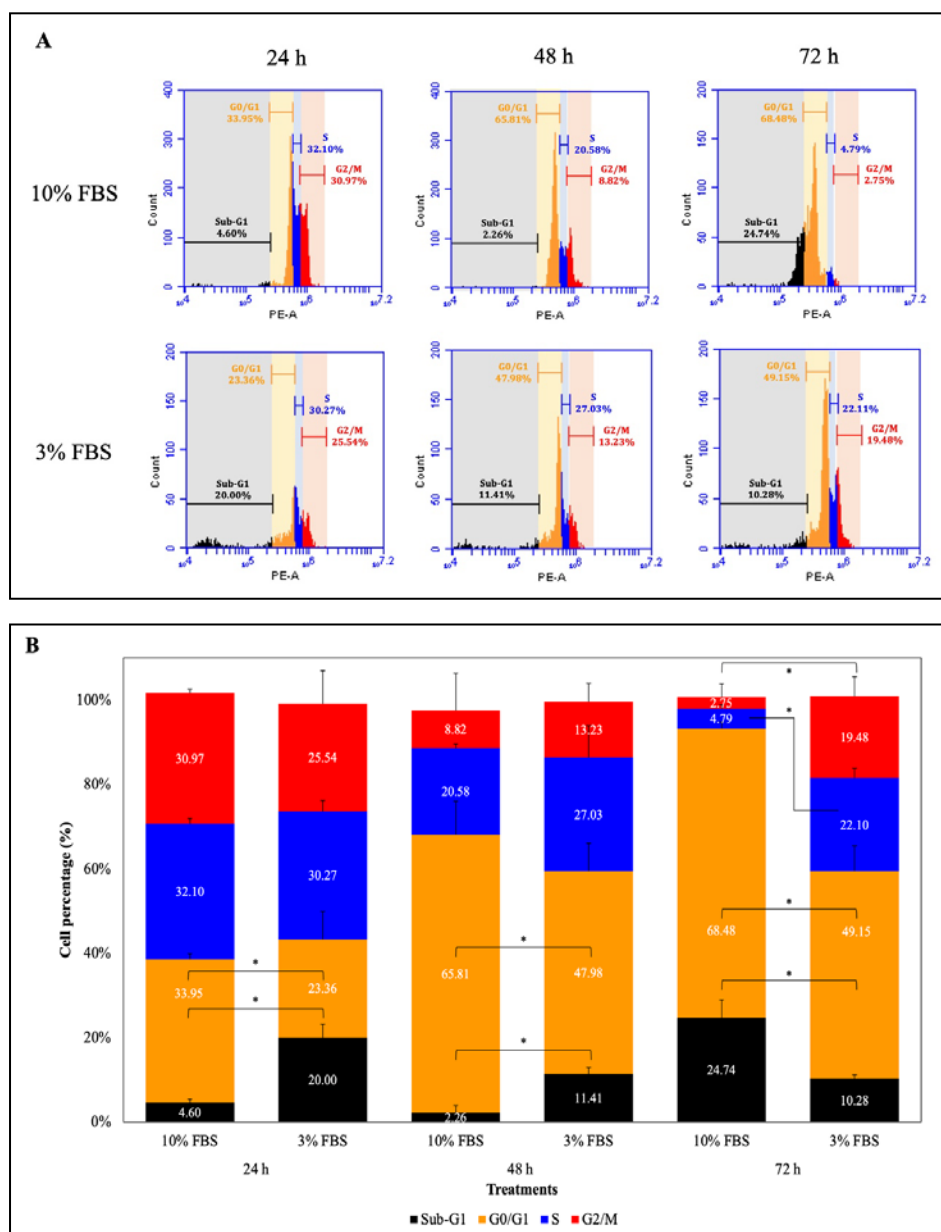
Figure 4. The cell cycle of clone RD8 supplemented with 10% and 3% FBS (n = 3). A. Flow cytometry-based cell cycle spectrum at 24 h, 48 h, and 72 h treatment. B. Cell percentage bar chart per cell cycle phase at 24 h, 48 h, and 72 h treatment. The percentage value is the geometric mean, and the system control value subtracts the relative percentage of cells. The cell cycle spectrum of hybridoma is divided into Sub-G1, G0/G1, S, and G2/M phases with different colour representatives. Cell cycle data were also statistically analyzed using the Mann-Whitney test. *($p \leq 0.05$).

In contrast to clone SB4, the cell cycle of clone RD8 supplemented with 10% FBS resulted in a lower population percentage of dead cells (sub-G1 phase) than in 3% FBS, especially at 24 h and 48 h (see Figure 4). The G0/G1 phase of both FBS percentages increased from 24 h to 72 h. Similarly, there was a gradual decrease in the percentage of cells in the S phase from 24 h to 72 h in both FBS percentages. However, a similar trend, as shown in SB4 cells (Figure 3), was also found in RD8 cells at 72 h. RD8 cells supplemented with 3% FBS showed a lower population of dead cells and a higher population of proliferating cells than those cultured with 10% FBS.

3.4. SDS-PAGE profile of mAbs

Figure 5 shows the presence of IgG heavy chains between 55–70 kDa and IgG light chains at ~25 kDa across

the sample. The heavy and light chains on mAbs from both clones with 3% FBS supplementation were clearly illustrated and thinner than those with 10% FBS. In addition, bands of 25 and ~70 kDa were detected in the flowthrough column. This indicates that the FBS supplementation also introduces proteins with sizes of 25 and ~70 kDa, similar to the light and heavy chains of mAbs. On the other hand, when mAbs concentrate is carried out using Amicon® Ultra-15 centrifugal filters 100 kDa MWCO (Merck Millipore Ltd, Germany), there are mAbs proteins carried over and detected in the flowthrough column and impurity proteins on the mAbs column. The impurity protein profile in 3% FBS supplementation is smaller than in 10% FBS.
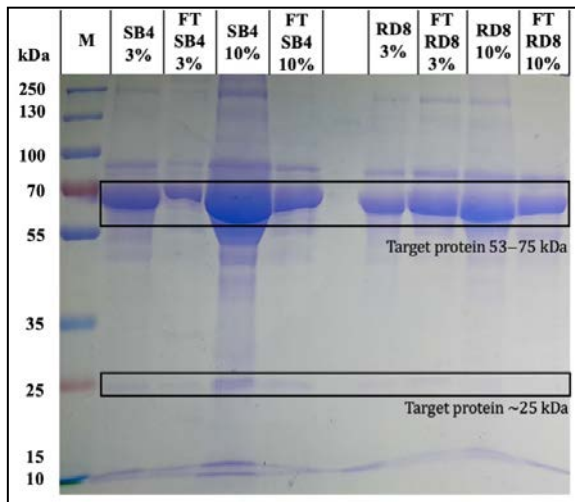
Figure 5. The SDS-PAGE result shows the protein profile of mAbs concentrate from clones SB4 and RD8 and the flowthrough sample collected after centrifugal separation (FT). Equal amounts of protein were loaded into wells of 10% resolving gel for separation (1 mg/well). The shape of the square indicates the target proteins, respectively. M: Marker; FT: Flow Through.

4. Discussion and Conclusion

Our results regarding the viable cell number of RD8 cultivated with 3% FBS are lower than those in a medium with 10% FBS. The decrease in cell proliferation in mammalian cells may occur due to a restricted glucose supply, as the FBS content is also reduced (Silva *et al.*, 2018; Pilgrim *et al.*, 2022). However, insignificant differences in growth kinetics between SB4 cells supplemented with 10% and 3% FBS indicate an adaptation process.

The calculation of the kinetics of SB4 cells in 3% FBS showed that PDT takes almost 7 hours longer than the cells cultivated with 10% FBS (Lindström and Friedman, 2020). This suggests that cells in 3% FBS have a slower growth rate than cells in 10% FBS since the growth rate is inversely correlated to the PDT (Shahrezaei and Marguerat, 2015). A long PDT and slow growth rate are also observed in RD8 cells cultivated in 3% FBS. The growth rate value represents the cell adaptability process (Lindström and Friedman, 2020) and the speed at which the cell population size changes over time.

The low serum content in the medium also results in a lower accumulation of metabolic waste products, as cell proliferation slows down (Konakovsky *et al.*, 2016; Jang *et al.*, 2022). This can be observed in microscopic observations (Figure 2) and supported by cell cycle analysis (Figures 3 and 4). The peak density of hybridoma supplemented with 10% FBS on day 3 indicates population dominance of mortality, thereby increasing apoptosis (sub-G1 phase) and low proliferating cells phase (G2/M phase) (Schellenberg *et al.*, 2022). In contrast, both SB4 and RD8 cells cultivated in 3% FBS showed a small proportion of sub-G1 phase cells and a more significant population of proliferating cells.

Cell growth shown in the results of cell kinetics is supported by cell cycle profile testing, which also describes the period of cell growth and multiplication (Eastman *et al.*, 2020). In the first 24 h, the cell density of SB4 and RD8 clones in 3% FBS media decreased compared to 10% FBS. This was also shown in the decrease in the percentage of the S phase in both clones at 24h due to the inhibition of cell proliferation by inducing G1 cycle arrest. Thus, cells were inhibited from entering the S or G2/M phase. This inhibition is probably caused by the interaction of CycE and CDK2 in the restriction G0 / G1, which is inhibited (Finn *et al.*, 2016; Fisher and Krasinska, 2022) due to growth factor deficiency and DNA damage, thus promoting cell cycle arrest to allow DNA repair to prevent the propagation of cells with severe DNA damage (Junqueira, 2003; Ozaki and Nakagawara, 2011; Yam *et al.*, 2022).

In contrast to proliferation capacity, reducing FBS supplementation significantly reduces the mAbs produced by SB4 cells. The peak of mAbs production occurs on the day when cell density reaches the highest number because the cell has been in the stationary phase and reached the maximum capacity of mAbs production (Lee and Palsson, 1994; Carvalho *et al.*, 2017), so mAbs production on the day of measurement after that is relatively constant. Meanwhile, the mAbs produced by RD8 cells grown with 3% FBS are not significantly different from those cultivated with 10% FBS. Thus, a low-serum medium may also facilitate mAbs production by RD8 cells. If a comparison is made to determine the productivity of each clone in a low-serum medium (according to Table 1), clone RD8 appears to be excellent in aspects of mAbs production. It is also supported by shorter PDT and has a faster growth rate than clone SB4.

The difference in mAbs production between these two clones is statistically significant. Each SB4 and RD8 clone is developed from B lymphocytes isolated from different mice. Thus, differences in physiological conditions and immunization outcomes may affect the cell's characteristics (Leenaars and Hendriksen, 2005). The various types of antigens in the isolation procedure of B lymphocytes of the two clones also affect the number of specific antibodies produced (Leenaars, 1994; Pedrioli and Oxenius, 2021). Furthermore, protocol aspects and fusion outcomes affect the monoclonality of hybridoma cells, potentially resulting in differences in the capacity to produce antibodies (Holzlohner and Hanack, 2017).

The pattern of the cell cycle may be associated with a non-constant rate of mAbs production, reaching a maximum in the S phase and decreasing gradually from the late S phase to the G2 phase until it reaches a minimum in the M phase (Grilo and Mantalaris, 2019). In addition, RD8 cells with 3% FBS showed a large percentage in the S phase, possibly due to the excellent adaptation process. Moreover, these adaptation processes also induce shorter G1 arrest cycles at 3% FBS, resulting in a relatively more significant number of cells in the G2/M (4n) phase than cells grown with 10% FBS. The S and G2/M phase cell percentage at 3% supplementation was better in clone RD8 than in clone SB4.

The mitotic phase in a 3% FBS low-serum medium is favourable compared to 10% FBS, particularly at the 72-hour observation point. This is attributed to the lower FBS concentration, where a longer duration of cell or serum starvation can increase the proportion of cells arrested in the G0/G1 phase (Huang *et al.*, 2018; Wang and Saponaro, 2021), although some studies have reported a non-significant increase (Baghdadchi, 2013). The increase in

the proportion of cells in the G0/G1 phase in the low-serum medium may lead to an improvement in cell quality during the mitotic phase through mTOR activation for adaptation and cellular repair (Bhowmick *et al.*, 2024) and DNA repair (Chae *et al.*, 2021). However, this could also be influenced by the characteristics of the hybridoma clone.

The result of SDS-PAGE analysis also showed the pattern of IgG profile produced by both clones. The antibodies, mainly IgG, are large molecules with a total weight of approximately 150 kDa, consisting of four polypeptide chains with two identical heavy chains of 53−75 kDa and two light chains of ~25 kDa (Rižner, 2014; Saied *et al.*, 2022). The visualization of impurity proteins included in mAbs production in 3% FBS shows less impurity compared to 10% FBS. Thus, this may facilitate mAbs purification (Pilgrim *et al.*, 2022). Meanwhile, the presence of protein bands in the flowthrough is likely to come from impurity proteins carried over from the FBS and from the mAbs sample triggered by the less-than-optimal effectiveness of Amicon concentration, so that the target protein is carried over to the flowthrough. Implementing Amicon 100k RC aims for reduced particle recovery. However, there is a possibility that the loss of particles was drastic and carried over to the flowthrough (Vergauwen *et al.*, 2017; Tang *et al.*, 2024).

Overall, the productivity of clones SB4 and RD8 in low-serum did not show a significant decrease compared to 10% FBS, which may still be sufficient to support mAbs production. Lastly, hybridoma clone RD8 has excellent adaptation to low-serum medium. However, the metabolic traits of each clone remain unclear. The limitation of this research regarding measuring the growth kinetics of hybridomas is that each repeat was carried out at different times, which may give rise to variations in data. This limitation can be optimized in future research to make it more reproducible.

Acknowledgement

References

Baghdadchi N. 2013. The Effects of Serum Starvation on Cell Cycle Synchronization. *OSR Journal of Student Research.*, **1**(4).

Baker M. 2016. Reproducibility: Respect your cells! *Nature.*, **537**(7620): 433–435.

Bhowmick T, Biswas S and Mukherjee A. 2024. Cellular response during cellular starvation: A battle for cellular survivability. *Cell Biochem Funct.*, **42**(5): 1–11.

Bruce MP, Boyd V, Duch C and White JR. 2002. Dialysis-based bioreactor systems for the production of monoclonal antibodies - Alternatives to ascites production in mice. *J Immunol Methods.*, **264**(1–2): 59–68.

Carvalho LS, da Silva OB, de Almeida GC, de Oliveira JD, Parachin NS and Carmo TS. 2017. Production Processes for Monoclonal Antibodies. **Fermentation Processes.** IntechOpen Publisher, London.

Chae SY, Nam D, Hyeon DY, Hong A, Lee TD, Kim S, Im D, Hong J, Kang C, Lee JW, Hwang D, Lee SW and Kim HI. 2021. DNA repair and cholesterol-mediated drug efflux induce dose-dependent chemoresistance in nutrient-deprived neuroblastoma cells. *iScience.*, **24**(4): 102325.

Eastman AE, Chen X, Hu X, Hartman AA, Morales, AMP, Yang C, Lu J, Kueh HY and Guo S. 2020. Resolving Cell Cycle Speed in One Snapshot with a Live-Cell Fluorescent Reporter. *Cell Reports.*, **31**(12): 107804.

Finn RS, Aleshin A and Slamon DJ. 2016. Targeting the cyclin-dependent kinases (CDK) 4/6 in estrogen receptor-positive breast cancers. *Breast Cancer Res.*, **18**(1): 1–11.

Fisher D and Krasinska L. 2022. Explaining Redundancy in CDK-Mediated Control of the Cell Cycle: Unifying the Continuum and Quantitative Models. *Cells.*, **11**(13).

Grilo AL and Mantalaris A. 2019. A Predictive Mathematical Model of Cell Cycle, Metabolism, and Apoptosis of Monoclonal Antibody-Producing GS–NS0 Cells. *Biotechnol J.*, **14**(11).

Groothuis FA, Heringa MB, Nicol B, Hermens JLM, Blaauboer BJ and Kramer NI. 2015. Dose metric considerations in in vitro assays to improve quantitative in vitro-in vivo dose extrapolations. *Toxicology*, **332**: 30–40.

Hashmi FK, Cail R, Islam M, Saleem Z, Amin U, Hussain K and Saeed H. 2014. Adaptation of WM-68 hybridoma cell-line in minimal serum and serum free culture conditions. *Pakistan J. Zool.*, **46**(2): 355–362.

Holzlohner. 2017. Generation by murine monoclonal antibodies by hybridoma technology. *J Vis Exp*, **119.**

Huang Y, Fu Z, Dong W, Zhang Z, Mu J and Zhang J. 2018. Serum starvation-induces down-regulation of Bcl-2/Bax confers apoptosis in tongue coating-related cells in vitro. *Mol Med Rep.*, **17**(4): 5057–5064.

Jang M, Pete ES and Bruheim P. 2022. The impact of serum-free culture on HEK293 cells: From the establishment of suspension and adherent serum-free adaptation cultures to the investigation of growth and metabolic profiles. *Front Bioeng Biotechnol.*, **10**(September): 1–16.

Junqueira. 2003. **Basic histology.** Mc Graw Hill Publisher, New York.

Khalil A. 2009. Inhibition of the in vitro growth of human mammary carcinoma cell line (MCF-7) by selenium and vitamin E. *Jordan J Biol Sci.*, **2**(1): 37–46.

Khan NT. 2023. Basics of Hybridoma Technology for the generation of monoclonal antibodies. *Anatomy Physiol Biochem Int J.*, **6**(3): 1–4.

Konakovsky V, Clemens C, Müller MM, Bechmann J, Berger M, Schlatter S and Herwig C. 2016. Metabolic control in mammalian fed-batch cell cultures for reduced lactic acid accumulation and improved process robustness. *Bioengineering (Basel).*, **3**(1).

Korzyńska A and Zychowicz M. 2008. A method of estimation of the cell doubling time on basis of the cell culture monitoring data. *Biocybernetics and Biomedical Engineering.*, **28**(4): 75–82.

Lee GM and Palsson BO. 1994. Monoclonal antibody production using free-suspended and entrapped hybridoma cells. *Biotechnol Genet Eng Rev.*, **12**(1): 509–533.

Leenaars M and Hendriksen CFM. 2005. Critical steps in the production of polyclonal and monoclonal antibodies: evaluation and recommendations. *ILAR J.*, **46**(3): 269–279.

Leenaars. 1994. **Adjuvants in laboratory animals.** Ponsen & Looijen publisher.

Lindström HJG and Friedman R. 2020. Inferring time-dependent population growth rates in cell cultures undergoing adaptation. *BMC Bioinformatics.*, **21**(1): 1–14.

Loniakan S, Rafiee A and Monadi A. 2023. Bacteroides Fragilis induce apoptosis and sub G1/G1 arrest via caspase and Nrf2 signaling pathways in HT-29 cell line. *Jordan J Biol Sci.*, **16**(2): 363–369.

Ningsih FN, Widayanti T, Sahlan M, Pramono AP and Pambudi S. 2023. The Effect of Indonesian Royal Jelly Supplementation on the Growth of Hybridoma and Its Monoclonal Antibody Production. *Proceedings of the 1st International Conference for Health Research – BRIN (ICHR 2022).*, **1**: 210–219.

Ozaki T and Nakagawara A. 2011. Role of p53 in cell death and human cancers. *Cancers.*, **3**(1): 994–1013.

Parveen S and Varalakshmi KN. 2022. BAX and P53 Over-Expression Mediated by the Marine Alga Sargassum Myriocystum leads to MCF-7, Hepg2 and Hela Cancer Cells Apoptosis and Induces In-Ovo Anti-Angiogenesis Effects. *Jordan J Biol Sci.*, **15**(2): 275–287.

Pedrioli A and Oxenius A. 2021. Single B cell technologies for monoclonal antibody discovery. *Trends Immunoly.*, **42**(12): 1143–1158.

Pilgrim CR, McCahill KA, Rops JG, Dufour JM, Russell KA and Koch TG. 2022. A Review of Fetal Bovine Serum in the Culture of Mesenchymal Stromal Cells and Potential Alternatives for Veterinary Medicine. *Front Vet Sci.*, **9**(May): 1–11.

Rižner TL. 2014. Teaching the structure of immunoglobulins by molecular visualization and SDS-PAGE analysis. *Biochem Mol Biol Educ.*, **42**(2): 152–159.

Saied ARA, Metwally AA, Alobo M, Shah J, Sharun K and Dhama K. 2022. Bovine-derived antibodies and camelid-derived nanobodies as biotherapeutic weapons against SARS-CoV-2 and its variants: A review article. *Int J Surg.*, **98**(January): 106233.

Salcedo N, Reddy A, Gomez AR, Bosch I and Herrera BB. 2022. Monoclonal antibody pairs against SARS-CoV- 2 for rapid antigen test development. *PLoS Negl Trop Dis.*, **16**(3): 1–19.

Saleh M, Ezz -din D and Al-Masri A. 2021. In vitro genotoxicity study of the lambda-cyhalothrin insecticide on Sf9 insect cells line using Comet assay. *Jordan J Biol Sci.*, **14**(2): 213–217.

Sánchez-Robles EM, Girón R, Paniagua N, Rodríguez-Rivera C, Pascual D and Goicoechea C. (2021). Monoclonal antibodies for chronic pain treatment: Present and future. *Int J Mol Sci.*, **22**(19): 1–26.

Schellenberg J, Nagraik T, Wohlenberg OJ, Ruhl S, Bahnemann J, Scheper T and Solle D. 2022. Stress-induced increase of monoclonal antibody production in CHO cells. *Eng Life Sci.*, **22**(5): 427–436.

Shahrezaei V and Marguerat S. 2015. Connecting growth with gene expression: Of noise and numbers. *Curr Opin Microbiol.*, **25**: 127–135.

Silva BG, da Silva Cunha Tamashiro WM, Ferreira RR, Deffune E and Suazo CAT. 2018. Assessment of kinetic and metabolic features of two hybridomas in suspension culture for production of two monoclonal antibodies for blood typing. *Braz J Chem Eng.*, **35**(2): 497–507.

Singer SR and McDaniel CN. 1986. Analyzing growth in cell cultures..I Calculating growth rates. *Can J Bot.*, **64**(1): 238–241.

Sissolak B, Lingg N, Sommeregger W, Striedner G and Vorauer-Uhl K. 2019. Impact of mammalian cell culture conditions on monoclonal antibody charge heterogeneity: an accessory monitoring tool for process development. *J Ind Microbiol Biotechnol.*, **46**(8): 1167–1178.

Tang S, Tao J and Li Y. 2024. Challenges and solutions for the downstream purification of therapeutic proteins. *Antib Ther.*, **7**(1): 1–12.

Urzì O, Bagge RO and Crescitelli R. 2022. The dark side of foetal bovine serum in extracellular vesicle studies. *J Extracell Vesicles.*, **11**(10).

Verderio P, Lecchi M, Ciniselli CM, Shishmani B, Apolone G and Manenti G. 2023. 3Rs principle and legislative decrees to achieve high standard of animal research. *Animals (Basel).*, **13**(2): 277.

Vergauwen G, Dhondt B, van Deun J, de Smedt E, Berx G, Timmerman E, Gevaert K, Miinalainen I, Cocquyt V, Braems G, van Den Broecke R, Denys H, de Wever O and Hendrix A. 2017. Confounding factors of ultrafiltration and protein analysis in extracellular vesicle research. *Sci Rep.*, **7**(1): 1–12.

Versteegen. 2021. Animal welfare and ethics on the collection of fetal bovine blood for the production of fetal bovine serum. *ALTEX.*, **38**(2).

Wang J and Saponaro M. 2021. Protocol for analysis of G2/M DNA synthesis in human cells. *STAR Protoc.*, **2**(2): 100570.

Yam CQX, Lim HH and Surana U. 2022. DNA damage checkpoint execution and the rules of its disengagement. *Front Cell Dev Biol.*, **10**(October): 1–15.